Title

The Apoptosis Repressor with a CARD Domain (ARC) Gene Is a Direct Hypoxia-Inducible Factor 1 Target Gene and Promotes Survival and Proliferation of VHL-Deficient Renal Cancer Cells

Journal

Molecular and Cellular Biology, 34(4)

ISSN

0270-7306

Authors

Razorenova, Olga V
Castellini, Laura
Colavitti, Renata
et al.

Publication Date

2014-02-01

DOI

10.1128/mcb.00644-12

Peer reviewed

Molecular and Cellular Biology

The Apoptosis Repressor with a CARD Domain (ARC) Gene Is a Direct Hypoxia-Inducible Factor 1 Target Gene and Promotes Survival and Proliferation of VHL-Deficient Renal Cancer Cells

Olga V. Razorenova, Laura Castellini, Renata Colavitti, Laura E. Edgington, Monica Nicolau, Xin Huang, Barbara Bedogni, Edward M. Mills, Matthew Bogyo and Amato J. Giaccia

Mol. Cell. Biol. **2014, 34(4):739. DOI: 10.1128/MCB.00644-12. Published Ahead of Print 16 December 2013.**

MCB
Journals.ASM.org

The Apoptosis Repressor with a CARD Domain (ARC) Gene Is a Direct Hypoxia-Inducible Factor 1 Target Gene and Promotes Survival and Proliferation of VHL-Deficient Renal Cancer Cells

Olga V. Razorenova,[a,b] Laura Castellini,[a] Renata Colavitti,[a] Laura E. Edgington,[c] Monica Nicolau,[d,h] Xin Huang,[e] Barbara Bedogni,[f] Edward M. Mills,[g] Matthew Bogyo,[c] Amato J. Giaccia[a]

Department of Radiation Oncology, Center for Clinical Sciences Research, Stanford University School of Medicine, Stanford, California, USA[a]; Department of Molecular Biology and Biochemistry, University of California, Irvine, California, USA[b]; Department of Pathology, Stanford University School of Medicine, Stanford, California, USA[c]; Department of Mathematics, Stanford University, Stanford, California, USA[d]; Magee-Womens Research Institute, Department of Obstetrics, Gynecology and Reproductive Science, University of Pittsburgh, Pittsburgh, Pennsylvania, USA[e]; Department of Biochemistry, Case Western Reserve University School of Medicine, Cleveland, Ohio, USA[f]; College of Pharmacy, The University of Texas at Austin, Austin, Texas, USA[g]; Department of Microbiology & Immunology, Baxter Laboratory for Stem Cell Biology, Stanford University School of Medicine, Stanford, California, USA[h]

The induction of hypoxia-inducible factors (HIFs) is essential for the adaptation of tumor cells to a low-oxygen environment. We found that the expression of the apoptosis inhibitor ARC (apoptosis repressor with a CARD domain) was induced by hypoxia in a variety of cancer cell types, and its induction is primarily HIF1 dependent. Chromatin immunoprecipitation (ChIP) and reporter assays also indicate that the *ARC* gene is regulated by direct binding of HIF1 to a hypoxia response element (HRE) located at bp −190 upstream of the transcription start site. HIFs play an essential role in the pathogenesis of renal cell carcinoma (RCC) under normoxic conditions, through the loss of the Von Hippel-Lindau gene (*VHL*). Accordingly, our results show that ARC is not expressed in normal renal tissue but is highly expressed in 65% of RCC tumors, which also express high levels of carbonic anhydrase IX (CAIX), a HIF1-dependent protein. Compared to controls, ARC-deficient RCCs exhibited decreased colony formation and increased apoptosis *in vitro*. In addition, loss of ARC resulted in a dramatic reduction of RCC tumor growth in SCID mice *in vivo*. Thus, HIF-mediated increased expression of ARC in RCC can explain how loss of *VHL* can promote survival early in tumor formation.

Hypoxia-inducible factors (HIFs) are oxygen-sensitive transcription factors that are essential for cellular adaptation to low-oxygen conditions. Increased expression of HIFs is observed in multiple cancers and has been reported to correlate with poor prognosis (1). Recent work has shown that HIFs regulate diverse aspects of malignancy, including glucose metabolism, angiogenesis, survival, proliferation, and differentiation (2). HIFs consist of an oxygen-sensitive alpha subunit, HIF1α or HIF2α, and a constitutively expressed beta subunit, HIF1β, also called ARNT (aryl hydrocarbon receptor nuclear translocator). Under atmospheric conditions (21% O_2), α HIFs are hydroxylated at proline residues (HIF1α at Pro402/564 and HIF2α at Pro405/531), are recognized by the E3-ubiquitin ligase VHL, and are targeted for proteasomal degradation. When oxygen levels decrease (5% O_2 or lower), HIF proteins remain nonhydroxylated, become stabilized, and bind to ARNT, forming a complex that orchestrates the transcriptional response to hypoxia. Alternatively, stabilization of α HIFs may occur even under normoxic conditions if VHL function is lost due to somatic mutations or epigenetic changes (e.g., promoter hypermethylation). *VHL* inactivation leading to increased HIFs levels and increased expression of HIF target genes has been detected in 80 to 90% of sporadic clear-cell renal-cell carcinomas (CC-RCCs), which account for the majority of renal cancers (3), and are notoriously resistant to cytotoxic chemotherapies. In the present study, we evaluated the *ARC* gene as a HIF target gene and investigated its contribution in renal tumorigenesis.

Over the past several years, studies have identified ARC, expressed primarily in heart, muscle, and brain, as a physiological mediator of apoptosis resistance (35). Unlike highly proliferative cells in the bloodstream, bone marrow, and gut, which have short life spans and high rates of apoptosis, differentiated postmitotic cells in the nervous system, heart, and skeletal muscle exhibit relative resistance to apoptosis to limit excess tissue degeneration in response to stress stimuli. The antiapoptotic action of ARC was originally attributed to its inhibition of caspases in skeletal muscle and heart through the interaction between its N-terminal caspase recruitment domain (CARD) and the homologous prodomains of apical caspases (4). ARC is implicated in the inhibition of both the intrinsic and extrinsic pathways of apoptosis (5). Recent work has shown that ARC may also promote apoptosis resistance through interactions with other proteins implicated in apoptotic pathway, including Fas and FADD (5). The extrinsic pathway is disrupted by the heterotypic binding between the CARD domain of ARC and the death domains of Fas and FADD, whereas the intrinsic pathway is impaired mainly by the interactions between ARC and the proapoptotic mediator Bax, which maintains Bax in its inactive conformation and prevents mitochondrial cytochrome *c* release (5, 6).

Although ARC expression is relatively low in most mammalian tissues, it is beginning to be recognized that its antiapoptotic func-

Received 16 May 2012 **Returned for modification** 10 June 2012
Accepted 18 November 2013
Published ahead of print 16 December 2013
Address correspondence to Amato J. Giaccia, giaccia@stanford.edu.
O.V.R., L.C., and R.C. equally contributed to this work.

doi:10.1128/MCB.00644-12

tion may be coopted in a variety of cancer cell types as part of an integral prosurvival mechanism during cancer development and maintenance. This hypothesis is strongly supported by the high prevalence of ARC expression in human cancers (7, 8) that increases the ability of cancer cells to inhibit apoptotic cell death in response to endoplasmic reticulum (ER) and mitochondrial stresses. For example, ARC was shown to inhibit ER stress-induced apoptosis in melanoma cells (9) and to contribute to resistance to doxorubicin-induced cancer cell death by inhibiting dynamin-related protein 1 (DRP1)-mediated mitochondrial fission (10). A recent study reported the role of ARC in stimulation of cancer cell proliferation in *in vivo* breast cancer model (11). In addition, ARC is highly expressed in leukemia, and its expression inversely correlates with patient survival (12). ARC can also promote tumor progression by impairing p53 function in breast cancer (13) and by cooperating with the Ras oncogene for the maintenance of the transformed phenotype (18).

In the past 5 years the mechanisms governing ARC expression have started to be elucidated. Studies by Nam et al. (15) and Foo et al. (16) have proposed a role for ubiquitination and proteasomal degradation in regulation of ARC protein expression. This mechanism of decreasing ARC protein levels would limit its antiapoptotic function in response to death stimuli. On the other hand, ARC expression is also negatively regulated at the mRNA level by p53, which blocked its expression under hydrogen peroxide treatment and anoxia, although the mechanism of this inhibition is poorly understood (17). In contrast, Ras acts as a positive regulator of ARC expression through stimulation of transcription and increased protein stability (18).

In this paper, we demonstrate that hypoxia, through the selective induction of HIF1α, is a key regulator of ARC expression in renal cancers with wild-type (WT) *VHL*. In addition, our data provide a mechanism for ARC overexpression in CC-RCC under normoxia, through the loss of *VHL* gene function and HIF1α upregulation. Further, ARC overexpression in RCC contributes to cell survival and growth, and ARC downregulation leads to cell death and decreased growth rate, suggesting that targeting ARC may be a useful therapeutic approach to control tumor growth.

MATERIALS AND METHODS

Cell cultures. A549, A375, MCF7, RCC4, RCC4-VHL, RCC10, RCC10-VHL, 786-0-VHL, A498-VHL, ACHN, SN12C, HeLa, TK10, HCT116, HCT116HIF1α$^{-/-}$, and 293FT cell lines were grown in Dulbecco's modified Eagle medium; Caki1 cells were grown in McCoy5a medium. Media were supplemented with 10% fetal bovine serum (Omega Scientific, Tarzana, CA), 2 mM L-glutamine, 100 U/ml penicillin, and 100 μg/ml streptomycin. Cells were grown in mixed-gas CO_2 water-jacketed incubators (21% O_2, 5% CO_2; Forma Scientific, Marietta, OH).

Hypoxic and anoxic treatment. Cells were plated in glass dishes, allowed to adhere for 16 to 20 h in a 21% O_2, 5% CO_2 incubator, and then transferred to an In Vivo$_2$ 400 hypoxic workstation (0.5% O_2 or 2% O_2; Biotrace Inc., Bothell, WA) or to a 0.02% O_2 Bactron anaerobic environmental chamber (Sheldon Manufacturing Inc., Cornelius, OR) for various times. The lysis of the cells for Western blotting was performed inside the chambers.

Western blotting. Cells were lysed directly on the dishes with ice-cold radioimmunoprecipitation assay (RIPA) buffer (50 mM Tris-HCl [pH 7.4], 150 mM NaCl, 1% NP-40, 0.1% SDS, 0.5% sodium deoxycholate) supplemented with Complete Mini protease inhibitors (Roche, Indianapolis, IN), kept on ice for 15 min, vortexed, and spun down at 14,000 × *g* (Eppendorf centrifuge 5415C). Total protein in the supernatant was quantified using a bicinchoninic acid (BCA) protein assay kit (Pierce, Rockford, IL), and 30 to 100 μg of protein per lane was separated on 10 to 12% bisacrylamide gels and then transferred onto 0.2-μm nitrocellulose membranes (Bio-Rad, Hercules, CA). The following primary antibodies were used to probe the membranes: rabbit antihemagglutinin (anti-HA) antibody (dilution, 1:2,000; Abcam Inc., Cambridge, MA), rabbit anti-ARC (dilution, 1:1,000; ab2002 and ab2003; Abcam), rabbit anti-HIF2α (dilution, 1:500; Novus Biological, Littleton, CO), mouse anti-HIF1α (dilution, 1:250; BD Biosciences, San Jose, CA), rabbit anti-ARNT (dilution, 1:1,000; BD Transduction Laboratories, San Jose, CA), rabbit anti-cleaved caspase 3 (dilution, 1:1,000; Cell Signaling, Danvers, MA), mouse anti-α-tubulin (dilution, 1:5,000; Fitzgerald Industries International, Concord, MA), mouse anti-β-actin (dilution, 1:5,000; Sigma-Aldrich, St. Louis, MO), mouse anti-HSP-70 (mitochondrial heat shock protein 70; dilution, 1:2,000; Thermo Scientific, Rockford, IL), and goat anti-mouse and goat anti-rabbit antibody conjugated to horseradish peroxidase (HRP; Zymed Laboratories Inc., South San Francisco, CA) or conjugated to alkaline phosphatase (AP; Vector Laboratories, Burlingame, CA). Western blot bands were quantified using the ImageJ (NIH) program.

Small interfering RNA (siRNA) and plasmid transfections. Cells were transfected according to the manufacturer's instructions with nontargeting siControl (siCTR), siHIF1α, siHIF2α, and siARNT smart pools (Dharmacon, Chicago, IL) using Dharmafect reagent 1 (Dharmacon). 293FT cells were transfected with pcDNA3, pcDNA3-HIF1α-CA-HA (P402A/P564A), or pcDNA3-HIF2α-CA-HA (P405A/P531A) (Addgene; deposited by W. G. Kaelin, Jr. [19, 20]) using Lipofectamine and PLUS reagents according to the manufacturer's instructions (Invitrogen).

Quantitative real-time PCR. Quantitative real-time PCR (QRT-PCR) was performed as described previously (21). Human TATA-binding protein (hTBP) primers were chosen as an internal control. Primer sequences are available upon request.

Chromatin immunoprecipitation assay. The chromatin immunoprecipitation (ChIP) assay was performed as described previously (22). RCC4 cells were fixed with 1% formaldehyde for 10 min at room temperature. Sonicated chromatin (70 to 100 μg) was incubated with rabbit anti-HIF-1α antibody (Abcam) or rabbit anti-HIF-2α antibody (Abcam), followed by precipitation with protein A/G Dynabeads (Invitrogen, Grand Island, NY). Alternatively, ChIP was performed on 293FT cells transiently transfected with pcDNA3 or pcDNA3-HIF2α-CA-HA (P405A/P531A) plasmids, 24 h posttransfection, using rabbit anti-HA antibody (Abcam). Relative enrichment was measured by QRT-PCR using a titration of pooled input samples as a standard curve. Normal rabbit IgG (Santa Cruz Biotechnology, Santa Cruz, CA) was used as a nonspecific IgG control, and the relative enrichment obtained for the nonspecific IgG control was subtracted from the relative enrichment of the samples. The sequences of primers flanking hypoxia response element 1 (HRE1) and HRE2 sites in ARC promoter were 5′GGGGAGGGAAAGCTGACTAC3′ and 5′CTGGGAATAGGGAGGGTGAG3′. Primers flanking jumonji domain-containing protein 1A (JMJD1A) HRE (5′TCCTTCAAAATGGCG GACTT3′ and 5′GCTGCTGGGCGAAATGG3′) and primers flanking ARRDC3 HRE (23) were used as positive controls, and primers upstream of ARC HRE1 and HRE2 located at bp −861 of the transcription start site were used as a negative control (5′CTGAAGAAAGGAGGGGGAAC3′ and 5′GCCCAAGTAGGAGGCAGTC3′).

Reporter plasmid construction, transient transfection, and luciferase assay. A region of DNA, 1,005 bp, containing an *ARC* promoter, exon 1, and a part of intron 1 (bp −701 to +304, where +1 corresponds to a transcription start site; the sequence and intron-exon structure of *ARC/Nol3* gene were obtained from the UCSC Genome Browser, human, February 2009 [GRCh37/hg19 assembly]) was synthesized and cloned in pUC57 by GenScript USA Inc., Piscataway, NJ. This DNA region was subsequently subcloned by NheI and XhoI into the vector pGL3-basic upstream of the firefly luciferase gene by PCR, using forward 5′AGAGA GGCTAGCAAGGGGCTTGGAACCAGTCC3′ and reverse 5′CTCTCTC TCGAGGTGCGACTGCACGGATTTTC3′ primers. The reporter plas-

mids mutated at the HRE1 (bp −106; CACGT) and HRE2 (bp −190; ACGTG) sites alone or in combination were constructed by site-directed mutagenesis using a QuikChange Lightning Multi site-directed mutagenesis kit from Stratagene (La Jolla, CA) according to the manufacturer's instructions with primers targeting HRE1 and HRE2, respectively (5′AG GCCCTGAGTGGGCGCTGGAAAAATGGGGCCGCGGGCCGAAC TG3′ and 5′AGGCCGCGCGCTGGCTGGGGATTTTCATGTAGTCAG CTTTCCCTC3′). All constructs were verified by sequencing. Reporter plasmids were transiently transfected to 293FT or TK10 cells using Lipofectamine and PLUS reagents accordingly to the manufacturer's protocol (Invitrogen). Twenty-four hours after transfection, cells were exposed to 0.5% O_2 for 17 h. The luciferase activity was measured by a Bright Glo luciferase assay kit (Promega BioSystems, Sunnyvale, CA) on a Monolight 2010 luminometer (Analytical Luminescence Laboratory). Relative luciferase units in all samples were normalized to the amount of protein in each lysate measured by BCA assay (Pierce).

shRNA and cDNA expression constructs, lentivirus packaging and infection of target cells. pLKO.1shARC no. 1 and no. 2 were obtained from Open Biosystems, Huntsville, AL. The target sequences in ARC mRNA are 5′GCCACACACATCATTGTCATT3′ for short hairpin RNA (shRNA) no. 1 and 5′GCATTGGATGCACTGCCTGAT3′ for shRNA no. 2. pLKO.1shGFP was a kind gift from Silvestre Vicent (Stanford University). To conduct simultaneous expression of shRNA constructs in pLKO .1-puro vector and cDNA constructs in pLM-CMV-H4-puro-PL3 vector, we replaced the puromycin resistance gene in the pLM-CMV-H4-puro-PL3 vector with a neomycin resistance gene by PCR using forward primer 5′AGAGAGACTAGTATGATTGAACAAGATGGATT3′ and reverse primer 5′TCTCTCGTCGACTCAGAAGAACTCGTCAAGAA3′ and subsequent cloning by SpeI and SalI sites. shRNA-insensitive ARC (sh-in-ARC) cDNA was synthesized by GenScript using a sequence template corresponding to WT human ARC (GenBank no. BC012798.2) with mutations mostly in the third positions of codons corresponding to the region targeted by shRNA no. 1 (GCATTGGATGCACTGCCTGAT → GCccTGGAcGCcCTaCCaGAc) and with a truncated 3′ untranslated region, which was targeted by shRNA no. 2. The WT amino acid sequence was preserved. The sh-in-ARC cDNA was subcloned from pUC57 to pLM-CMV-H4-neo-PL3 by NheI and XhoI sites. Lentivirus production and infections were done as described previously (24). Infected cells were selected in puromycin-containing medium (1 to 2 μg/ml) or neomycin-containing medium (350 μg/ml) for 1 week.

Analysis of patients' data. Data were obtained based on two public gene expression microarray data sets: 177 tumor tissue samples and 10 renal cortex normal tissue samples (25, 26). cDNA data from Higgins et al. (25) and Zhao et al. (26) were extracted using Stanford Microarray Database (SMD) packages, and then data were transformed using disease-specific genomic analysis (27) for ARC: Hs.513667 UniGene build 207. Data were initially processed using SMD preprocessing, with a spot regression correlation greater than 0.5 and signal/background intensity greater than 1.5; only genes with 80% good data were retained, and then data were collapsed by UniGene cluster ID build 207. Data were then transformed using the high-dimensional supervised method disease-specific genomic analysis, which produces a high-dimensional healthy-state model, estimated from the normal tissue data, and then transforms each tumor vector to measure deviation from the healthy state. The healthy-state model is constructed in the original space whose dimension is the number of genes in the original microarray data, and for the present analysis the dimension of the healthy-state model was reduced to 24. An estimate of healthy-tissue values was obtained through a leave-one-out procedure performed on normal tissue data, as explained by Nicolau et al. (27). The values for each gene measure the extent to which the gene deviates from the healthy state. Thus, the measures for normal tissue—the leave-one-out values—give an estimate of significance: values in tumors are significant if they exceed the leave-one-out estimates computed for normal tissue. This estimate can be computed using the collection of values for a single gene in all normal tissue, or using all genes in all normal tissue. Since there are only 10 normal tissue samples, the latter provides a distribution based on a larger sample size for estimating significance. Specifically, we compared the distribution of data from ARC (Hs.513667) in 177 tumors to two distributions: one was distribution of ARC in the normal tissue, and the other was the distribution of all genes in the normal tissue. The former compares specifically the levels of ARC in normal and tumor tissues. The latter compares ARC in tumors to all genes in normal tissue.

Immunohistochemistry. Kidney cancer tissue arrays were purchased from US Biomax, Rockville, MD. Antigen retrieval was performed as described previously (21). The slides were incubated overnight at 4°C with a primary rabbit anti-ARC antibody (dilution, 1:400; ab2002; Abcam Inc., Cambridge, MA), mouse anti-CAIX (dilution, 1:100; Bayer, Elkhart, IN), or rabbit anti-cleaved caspase 3 (dilution, 1:300; 9661; Cell Signaling) followed by biotinylated secondary anti-rabbit or anti-mouse IgG (Santa Cruz Biotechnology) and finally with HRP-conjugated streptavidin (Calbiochem, Gibbstown, NJ). The target proteins were visualized with an AEC chromogen kit (Lab Vision, Fremont, CA) and counterstained in hematoxylin solution. Slides were analyzed using a Leica DM6000B microscope (Leica Microsystem Inc., Bannockburn, IL) under ×40 and ×20 magnification. Each spot was scored as negative or positive depending on the intensity of the staining. Since *VHL* loss occurs in 80% of all RCC tumors, HIF target genes get uniformly upregulated throughout the tissue section: the majority of cancer cells stain positively, and stromal cells stain negatively.

Cell proliferation assay. Cells stably expressing shRNA targeting green fluorescent protein (shGFP), shARC no. 1, or shARC no. 2 were counted with a Coulter Z1 particle counter (Beckman Coulter, Fullerton, CA), and 10^5 cells were plated in triplicate in 60-mm dishes, allowed to adhere overnight in a 21% O_2, 5% CO_2 incubator, subjected to normoxic (21% O_2) or hypoxic (0.5% O_2) conditions as described above, and counted and replated every third day for a period of 2 weeks.

Colony survival assay. Cells were counted and seeded in 60-mm dishes at 3,000 cells/dish (Caki1 cells), 1,000 cells/dish (RCC4 and RCC4-VHL), and 300 cells/dish (RCC10 and RCC10-VHL) in triplicate and subjected to normoxic (21% O_2) or hypoxic (2% O_2) conditions for the duration of the colony assay or to 0.5 μg/ml cisplatin or vehicle control pretreatments for 17 h before the colony assay, as indicated in the corresponding figures. After 2 weeks, colonies were fixed and stained with 95% ethanol and 0.1% crystal violet solution and manually counted.

Detection of caspase 3 activity with fluorescent probes. The detailed protocol is described in reference 28. In brief, Caki1 cells expressing shGFP, shARC no. 1, and shARC no. 2 were either treated with caspase inhibitor Z-VAD-FMK at 20 nM or left untreated for 48 h. Cell lysates were labeled with caspase probe LE22 and resolved on 15% bisacrylamide gel. Fluorescence was detected at Typhoon scanner with Cy5 laser (excitation/emission, 630/670 nm).

Annexin V-PI staining. Apoptosis was assayed by staining the cells with the fluorescein isothiocyanate (FITC)-annexin V apoptosis detection kit (BD Biosciences) according to the manufacturer's instructions. Briefly, 72 h after seeding, both adherent and nonadherent cells were collected. A total of 10^6 cells were incubated with FITC-annexin V and propidium iodide (PI) and analyzed by flow cytometry using a FACScan (Becton, Dickinson). The percentage of FITC-annexin V-positive and PI-negative cells (i.e., early apoptotic cells) was used to compare apoptotic rates in the cell lines analyzed. The percentage of apoptotic cells was analyzed using CellQuest software (BD Biosciences).

***In vivo* experiments.** Male SCID (B6.CB17) mice supplied by Charles River Laboratories International Inc. (San Diego, CA) were housed in an APLAC-approved facility at Stanford. Caki1 cells stably expressing shGFP, shARC no. 1, or shARC no. 2 were detached by trypsin, washed in 1× phosphate-buffered saline (PBS), and counted, and 3×10^6 trypan blue-negative cells in 100 μl 1× PBS were injected subcutaneously into the right and left dorsal flanks of the mice. All mice were sacrificed 13 weeks after cell implantations; primary tumors were excised and mea-

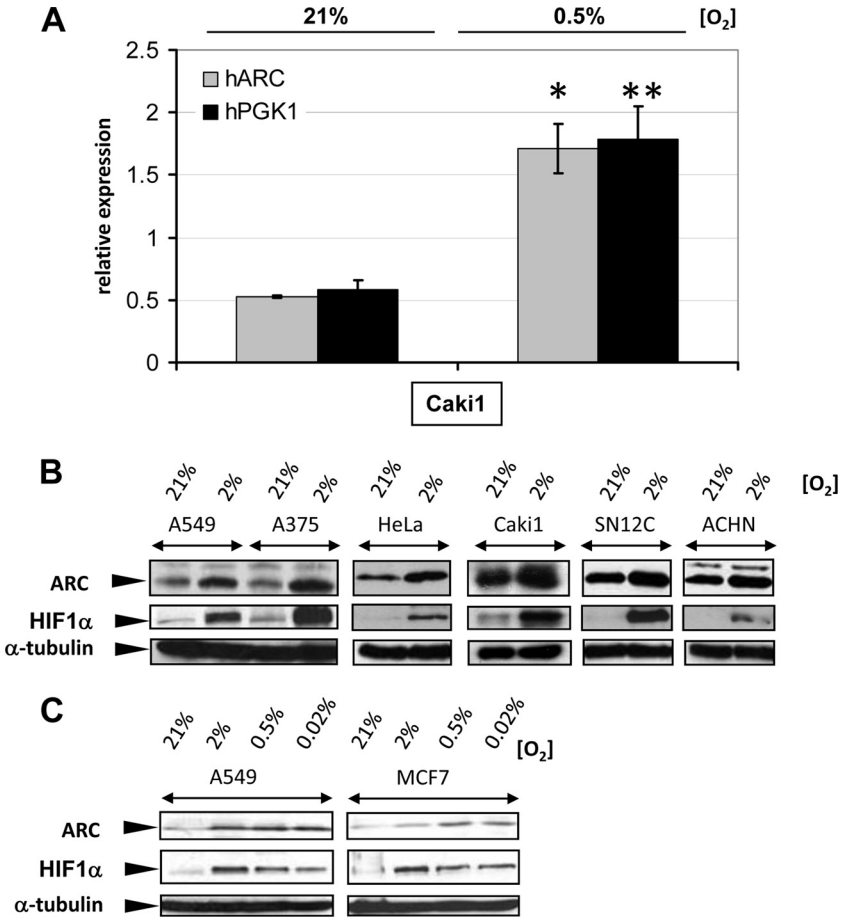

FIG 1 ARC expression is induced by hypoxia. (A) QRT-PCR showing induction of *ARC* and *PGK1* expression in Caki1 cells exposed to hypoxia for 16 h compared to normoxia. *TBP* expression was used as an internal control. The data represent the mean relative expression ± SEM from four independent experiments, each performed in triplicate. *, $P < 0.001$, and **, $P < 0.01$, compared to normoxia. (B) Western blots showing the ARC and HIF1α protein expression under normoxia or hypoxia in the indicated cancer cell lines. (C) Western blots, showing ARC and HIF1α protein levels in A549 and MCF7 cancer cell lines, under different oxygen tensions. In panels B and C, α-tubulin is shown as a loading control.

sured with calipers. Tumor volume was calculated using the following formula: width^2 × length × 0.5.

RESULTS

ARC is induced by hypoxia in tumor cells. ARC is expressed in cancer cell lines of different tissue origins even though it is not represented in their normal counterparts (7, 8). We confirmed the presence of ARC in a collection of lysates coming from melanoma (A375), lung (A549), cervix (HeLa), breast (MCF7), and renal (Caki1, SN12C, ACHN, and RCC4) carcinoma cell lines (data not shown). Moreover, while systematically analyzing a microarray of hypoxia induced genes in renal cancer cells, previously published by our group (22), we found the expression of *ARC* to be induced by exposure to 0.5% O_2. To confirm the induction of *ARC* by hypoxia in renal cancer, we used Caki1 cells, which express a WT *VHL* gene at a lower level than other WT *VHL* RCC cell lines (29) and respond to hypoxia by inducing HIF stabilization and activation. We subjected Caki1 cells to hypoxia (0.5% O_2, 16 h) and normoxia (21% O_2) and assessed *ARC* expression at the mRNA level by quantitative real-time PCR (QRT-PCR). *ARC* mRNA exhibited hypoxic induction similar to that of a well-known HIF1α target gene encoding phosphoglycerate kinase 1 (*PGK1*) (30) (Fig. 1A). Moreover, we found ARC protein to be induced by hypoxia in cell lines of diverse histological origins, such as A549 (non-small-cell lung carcinoma), A375 (melanoma), HeLa (cervical cancer) (Fig. 1B), Caki1, SN12C, ACHN (renal cancer) (Fig. 1B), and MCF7 (breast cancer) (Fig. 1C) cell lines. Furthermore, hypoxic inducibility of ARC protein could be detected at oxygen levels ranging from 2% to 0.02% (anoxia) (Fig. 1C).

The hypoxic induction of ARC in CC-RCC is dependent on HIF1α activation. Since hypoxia induced *ARC* expression at the mRNA level, we investigated whether *ARC* was regulated through HIF transcription factors (2). We used RCC4-VHL, 786-0-VHL, and A498-VHL cells, which are derivatives of *VHL*-deficient RCC4, 786-0, and A498 cells respectively, which were stably transduced with WT *VHL*. Stable transduction of *VHL* resulted in destabilization of α HIFs in normoxia and restoration of their inducibility in hypoxia. We exposed these cell lines to normoxia (21% O_2) or hypoxia (2% O_2) for 16 h and found that while RCC4-VHL cells (expressing both HIF1α and HIF2α) showed induction of ARC protein by hypoxia, 786-0-VHL and A498-VHL cells (expressing HIF2α but not HIF1α) failed to induce ARC (Fig. 2A). These results suggested that *ARC* was regulated by HIF1α under

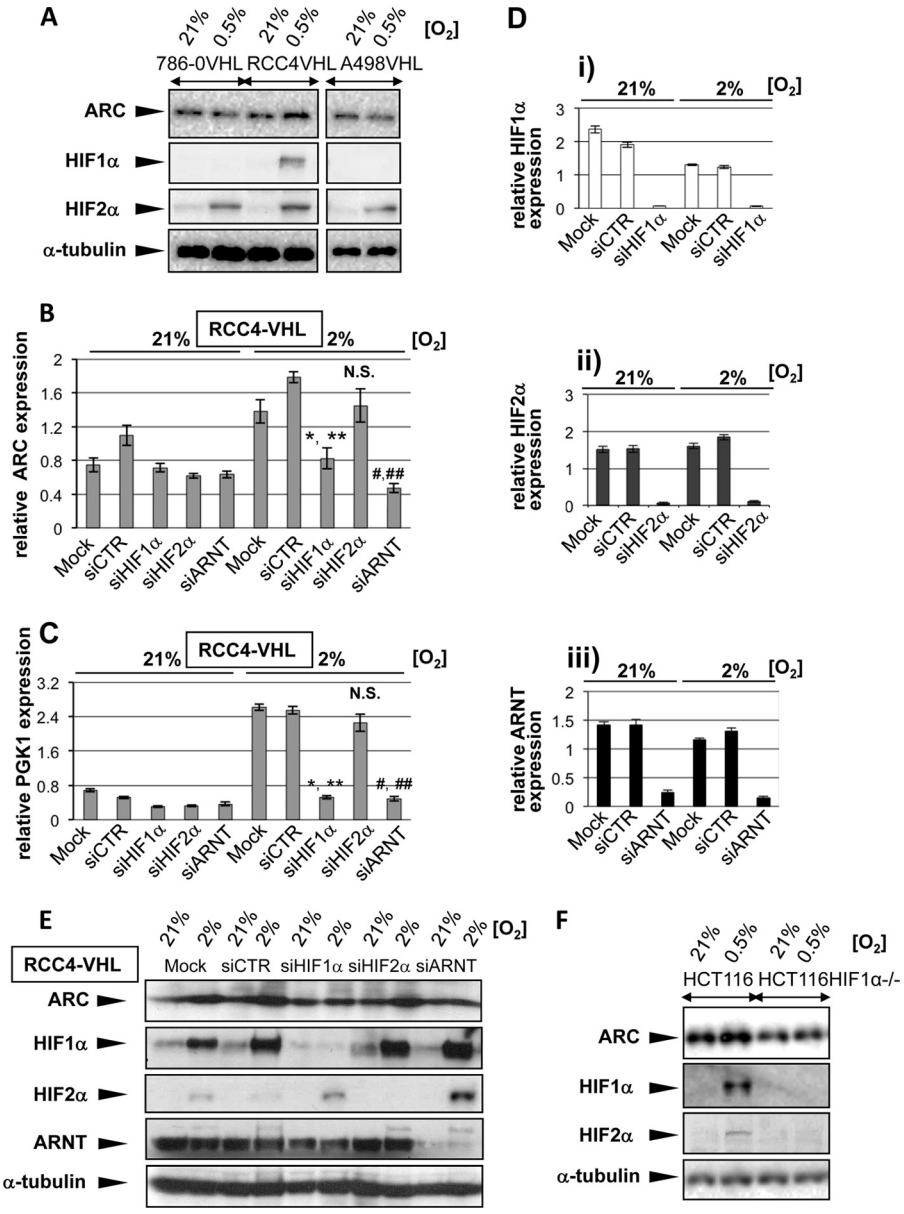

FIG 2 Hypoxic induction of ARC is HIF1α dependent. (A) Western blot showing hypoxic induction of ARC and HIF1α in RCC4-VHL cells but not in 786-0-VHL or A498-VHL cells, which lack HIF1α expression. (B) QRT-PCR showing the expression of *ARC* mRNA in RCC4-VHL cells transiently transfected with siRNAs targeting *HIF1*α, *HIF2*α, *ARNT*, or nontargeting control siRNA (siCTR) and exposed to normoxia or hypoxia. *ARC* induction by hypoxia is ablated when either the siRNA for *HIF1*α or *ARNT* is used but is unaffected by siRNA for *HIF2*α. *, $P < 0.05$; ** and #, $P < 0.01$; ##, $P < 0.001$. (C) QRT-PCR showing the induction of a known HIF1α target gene (*PGK1*) by hypoxia and abrogation of its induction in response to *HIF1*α or *ARNT* downregulation by siRNA transfections. * and #, $P < 0.0001$; ** and ##, $P < 0.001$. (B and C) * and #, comparison to mock transduced cells at 2% O_2; ** and ##, comparison to siCTR transduced cells at 2% O_2. (D) QRT-PCR showing downregulation of *HIF1*α (i), *HIF2*α (ii), and *ARNT* (iii) expression in RCC4-VHL cells 40 h after appropriate siRNA transfection (as indicated) under normoxia and hypoxia. (E) Western blot showing the impact of knocking down HIF1α, HIF2α, and ARNT in RCC4-VHL cells on ARC induction by hypoxia. (F) Western blot showing hypoxic induction of ARC and HIF1α in HCT116 cells but not in HCT116HIF1α$^{-/-}$ cells, which lack HIF1α expression. In panels A, E, and F, α-tubulin is shown as a loading control. In all panels, hypoxic exposure was for 16 h. In panels B to E, "mock-transfected" refers to samples with Dharmafect1 transfection reagent only, and siCTR is a nontargeting control siRNA. In panels B to D, *TBP* expression was used as an internal control, and the data represent the mean relative expression ± SEM from three independent experiments, each performed in triplicate.

hypoxic conditions. To confirm these findings, we used QRT-PCR to quantify changes in ARC expression in RCC4-VHL cells transiently transfected with siRNA duplexes targeting HIF1α, HIF2α, and ARNT or with nontargeting scrambled siRNA and exposed to normoxia (21% O_2) and hypoxia (2% O_2) for 16 h. ARNT is recruited by both HIF1α and HIF2α to form heterodimers that directly bind hypoxia response elements (HREs) in the regulatory sequences of hypoxia-dependent genes, and inhibition of ARNT results in decreased transcriptional activity of both HIF1α and HIF2α. Inhibition of *HIF1*α or *ARNT* expression repressed the induction of *ARC* by hypoxia, while the knockdown of *HIF2*α had little effect (Fig. 2B). We also confirmed that the induction of the

known HIF1α target *PGK1* (30) by hypoxia mirrored *ARC* induction and was also decreased in cells expressing *HIF1α* or *ARNT* siRNAs (Fig. 2C). To complement these data, we confirmed that each specific target gene was downregulated by the relative siRNA (Fig. 2D). Next, we monitored the induction of ARC by hypoxia at the protein level in response to HIF1α, HIF2α, and ARNT inhibition by siRNAs and confirmed that ARC hypoxic induction is specifically dependent on HIF1α (Fig. 2E). Finally, we showed that ARC is upregulated by hypoxia in HCT116 cells but not in HCT116HIF1α$^{-/-}$ cells (Fig. 2F).

HIF1α directly binds to HRE in *ARC* promoter located at bp −190 from the transcription start site. In order to determine if *ARC* was a direct HIF1 target gene, we conducted chromatin immunoprecipitation assays (ChIP). We used anti-HIF1α and anti-HIF2α antibodies and normal IgG (negative control) and chromatin derived from the RCC4 cells, where α HIFs are constitutively expressed under normoxia due to *VHL* loss. The strong HIF1- and HIF2-binding region was flanked with primers located adjacent to the transcription start site and contained two HREs: HRE1 (CACGT) at bp −106 and HRE2 (ACGTG) at bp −190 from the transcription start site (Fig. 3A). Primers flanking the JMJD1A HRE and ARRDC3 HRE were used as positive controls (22, 23), and primers flanking an HRE located at bp −861 upstream of ARC transcription start site were used as negative controls. Interestingly, both HIF1α and HIF2α are capable of binding the HRE1-2 region in ARC promoter, but only in the case of HIF1 does this binding lead to ARC upregulation by hypoxia (Fig. 2). We further assessed whether HIF2 can contribute to ARC regulation by overexpressing the stable P405A/P531A mutant of HIF2α in 293FT cells. Figure 3B confirms that HIF2α binds to the promoter region of ARC (HRE1-2) in 293FT cells. Also, ARC expression is induced in 293FT cells overexpressing HIF1α or HIF2α (Fig. 3C). Since the two HREs identified are located close to each other, the resolution of ChIP was not enough to determine whether HIF bound one or both sites.

To determine which HRE site was the HIF binding site, we conducted an *ARC* promoter reporter assay. A 1,005-bp DNA region containing the *ARC* promoter, exon 1, and a part of intron 1 (bp −701 to +304, where +1 corresponds to a transcription start site) was cloned into pGL3-basic upstream of the firefly luciferase gene (Fig. 3D). We also generated reporter plasmids mutated at the HRE1 (CACGT to TTTTT) and HRE2 (ACGTG to ATTTT) sites alone or in combination (sequencing data not shown). To conduct the reporter assays, we used the cell line 293FT, which was established from immortalized human embryonic kidney cells. The choice of 293FT cells over RCC cells was based on their high transfection efficiency: RCC cell lines are notoriously hard to transfect. First, we confirmed the ARC induction by hypoxia in 293FT cells (Fig. 3E) (the average induction over normoxia is 1.76 times, as assessed by Western blotting densitometry; $P = 0.023$). 293FT cells are known to have mild hypoxic upregulation of HIF target genes, where a 5×HRE reporter construct (positive control containing 5 consecutive hypoxia response elements fused to luciferase) consistently displayed an average 6-fold induction in comparison to other cancer cell lines, which displayed up to a 170-fold induction of the same construct (data not shown). Next, reporter plasmids were transiently transfected into 293FT cells, which were subsequently exposed to 0.5% O_2 for 17 h or kept in 21% O_2. Comparison of luciferase activity in normoxia and in hypoxia for all those reporter constructs clearly shows that the HRE2 site (ACGTG at bp −190) is the HIF binding site, since mutations in this site completely disrupted the induction of the ARC promoter by hypoxia (Fig. 3F). These results were confirmed in the renal cancer cell line TK10, which is characterized by WT *VHL* expression (Fig. 3G).

ARC is highly expressed in human renal cell cancer, and its expression overlaps with the HIF1α target carbonic anhydrase IX (CAIX) gene. Given the HIF1α dependence of ARC expression in cancer cell lines, we hypothesized that ARC expression should be elevated in CC-RCC, where HIFs are stabilized in about 80% of cases as a consequence of *VHL* loss (3). The analysis of *ARC* expression in the Oncomine database revealed three studies (31–33) showing the elevation of *ARC* expression in renal cancer compared to normal kidney tissue (Fig. 4A to C). In addition, we analyzed microarray data to compare expression levels of ARC in RCC tumors and in normal kidney tissue. Data were obtained from two public gene expression microarray data sets containing 177 tumor tissue samples and 10 renal cortex normal tissue samples (25, 26). The distribution of data for *ARC* in tumors was compared to two distributions: one was the distribution of *ARC* in normal tissue, and the other was the distribution of all genes in normal tissue (see Materials and Methods for the detailed procedure). Box plots of ARC distribution are displayed in Fig. 4D and show that *ARC* is significantly prevalent in tumor tissue relative to normal tissue.

To assess ARC protein levels in renal tumors, we stained a human kidney cancer tissue microarray (TMA) and compared the expression of ARC with the HIF1α-regulated enzyme CAIX (34) on a serial section from the same TMA. We found that while the normal renal tissue samples were all negative for both ARC and CAIX staining, among 57 cases of RCCs, 37 stained positive for ARC and 47 stained positive for CAIX, with a 78.7% overlap between the two stainings (Fig. 4E and F).

ARC knockdown decreases cell survival and retards growth of renal cancer cells, especially under hypoxia. The high prevalence of ARC in RCC prompted us to investigate whether ARC acts in an antiapoptotic role in this type of cancer. To directly test the role of ARC in cell survival, we infected Caki1 cells with lentiviral constructs expressing two different shRNAs targeting ARC and with a lentiviral construct expressing shRNA targeting green fluorescent protein (shGFP) as a control. After puromycin selection, we obtained two cell lines with a stable downregulation of ARC protein of 53% and 77%, respectively, compared to shGFP-expressing control cells (assessed by Western blotting densitometry; $P < 0.0001$ for both). This downregulation was accompanied by an increase in caspase 3 cleavage (Fig. 5A) (the average induction of caspase 3 cleavage over shGFP-infected cells is 10.31-fold for shARC no. 1 and 22.54-fold for shARC no. 2, as assessed by Western blotting densitometry; $P = 0.036$ and 0.021, respectively). We also assessed caspase 3 activity using the fluorescent probe LE22 (28), which specifically binds to caspase 3 in an active conformation. We observed probe binding to caspase 3 in cells where ARC was knocked down but to a much lesser extent in shGFP-expressing cells (Fig. 5B). The binding was no longer detected when cells were incubated with caspase inhibitor Z-VAD-FMK. We also carried out annexin V-propidium iodide (PI) staining of shGFP-, shARC no. 1-, and shARC no. 2-expressing cells and observed a difference in the percentage of annexin V-positive, PI-negative cells (Fig. 5C). Those results suggest that ARC plays an antiapoptotic role in Caki1 cells.

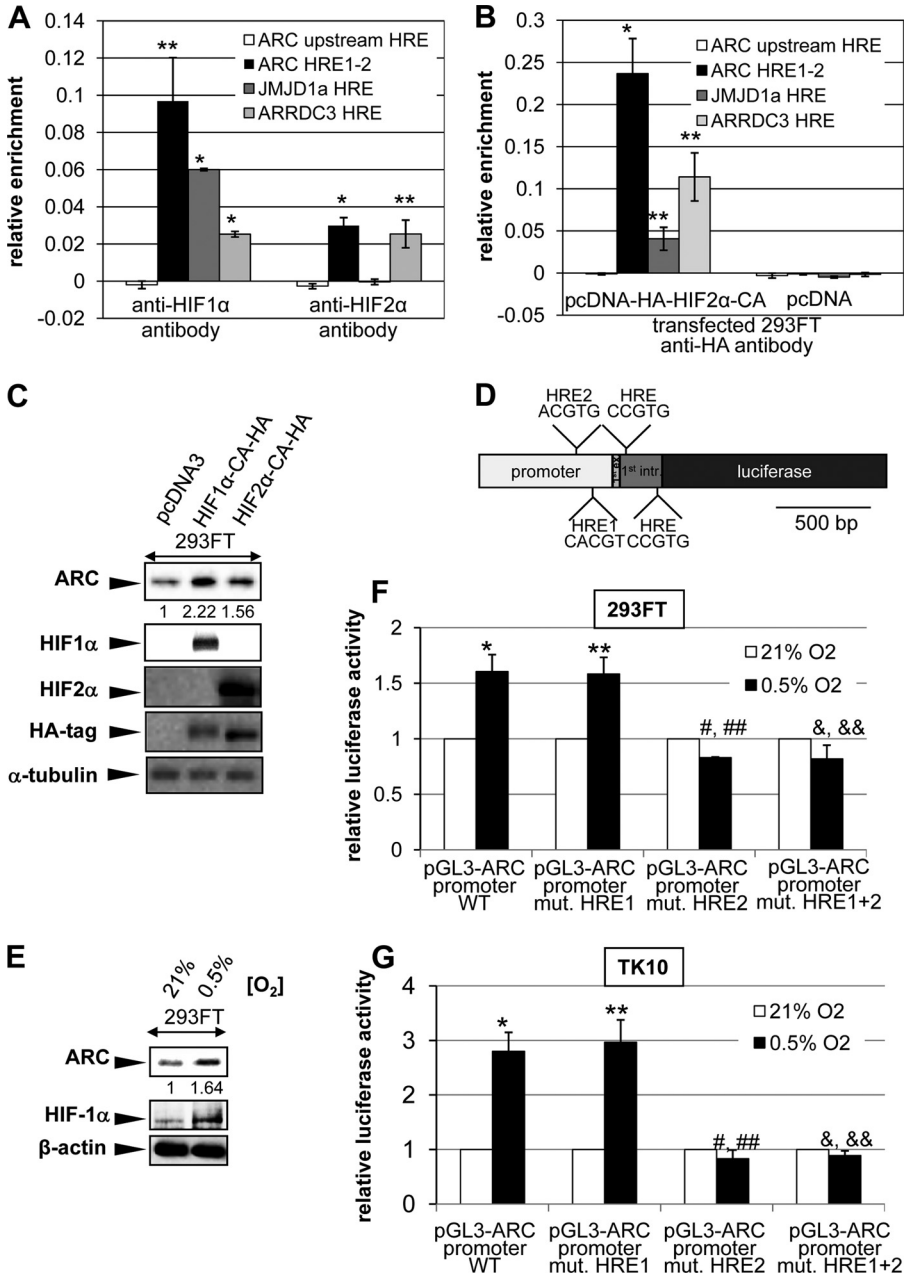

FIG 3 ARC is a direct HIF1α target gene. (A) HIF1α and HIF2α bind to the promoter region of *ARC* where two HREs (HRE1-2) are located. ChIP assays were performed on RCC4 cells with high levels of HIF1α and HIF2α under normoxia. (B) HIF2α binds to the promoter region of *ARC* (HRE1-2) in 293FT cells transiently transfected with pcDNA3-HIF2α-CA-HA (P405A/P531A). In panels A and B, JMJD1A and ARRDC3 HREs were used as a positive control, and HRE upstream of the ARC HRE1-2 region was used as a negative control. The graphs show mean relative enrichment ± SEM of two to three independent experiments, each performed in duplicate. *, $P \leq 0.01$, and **, $P \leq 0.05$, compared to *ARC* upstream HRE (negative control). (C) ARC expression is induced in 293FT cells overexpressing HIF1α or HIF2α. pcDNA3, vector control. (D) Schematic of the ARC reporter plasmid, containing the ARC promoter, exon 1, and a part of intron 1 located upstream of the firefly luciferase gene. HRE sites are indicated. (E) Western blot showing the ARC and HIF1α protein induction under hypoxia in the 293FT cell line. (F) Results of a reporter assay showing luciferase induction in 293FT cells transiently transfected with the promoter plasmid pGL3-ARC, as well as the promoter plasmid pGL3-ARC with mutated HRE1 upon hypoxic exposure for 17 h. The hypoxic induction is absent when HRE2 alone or in combination with HRE1 is mutated. * and &, $P \leq 0.01$; **, &&, #, and ##, $P < 0.05$. (G) Reporter assay showing luciferase induction upon hypoxic exposure for 17 h of TK10 cells transiently transfected with pGL3-ARC promoter plasmids with intact HRE2 site. *, **, #, ##, &, and &&, $P < 0.01$. (F and G) * and **, comparison to normoxia; # and &, comparison to fold induction of pGL3-ARC promoter in hypoxia; ## and &&, comparison to fold induction of pGL3-ARC promoter with mutated HRE1 in hypoxia. In panels F and G, luciferase activity under normoxia was designated 1, and the data represent the mean relative induction of luciferase activity and SEM for a minimum of two up to four independent experiments.

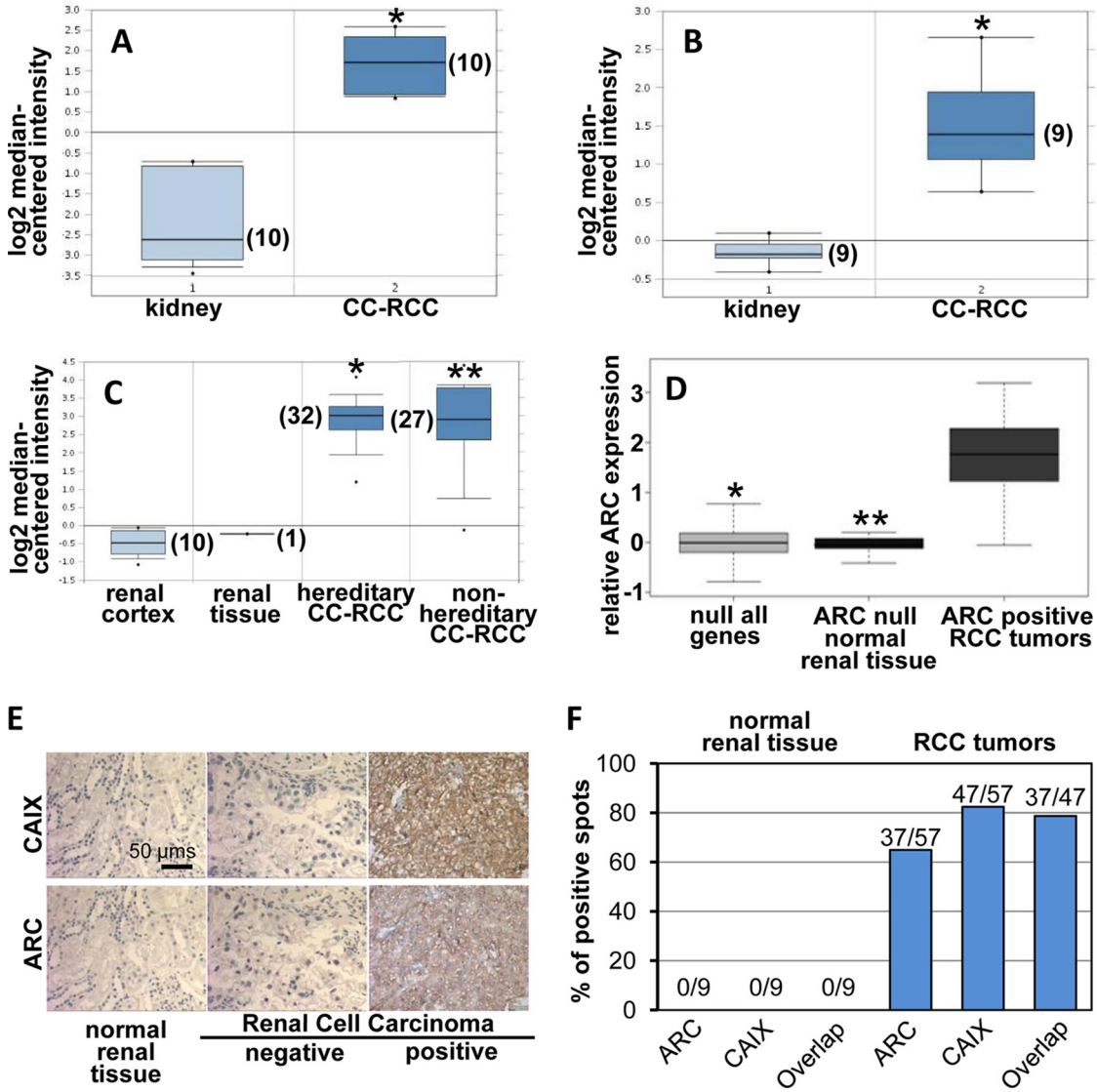

FIG 4 ARC is highly expressed in human RCC, and its expression overlaps with that of the CAIX gene (HIF1α target gene). (A to C) *ARC* mRNA expression is elevated in human RCC compared to normal renal tissue. Data were obtained from the Oncomine database. The number of samples in each group is shown in parentheses next to each box plot. (A) *, $P = 1.84E-8$; (B) *, $P = 1.58E-5$; (C) *, $P = 4.03E-23$; **, $P = 7.17E-16$. (D) ARC is significantly prevalent in tumor tissue relative to normal tissue. The box plot shows the distribution of data for ARC in tumors compared to two distributions, distribution of ARC in the normal tissue and distribution of all genes in the normal tissue. See Materials and Methods for the detailed procedure. *, $P < 2.2E-16$; **, $P = 2.3E-15$. (E) Representative photographs of ARC and CAIX immunohistochemical (IHC) staining on the tissue microarray (TMA). Examples of negative normal renal tissue staining and negative and positive RCC tumor staining are shown. (F) Quantitation of the IHC staining shown in panel E.

While Caki1 cells express a low level of WT *VHL* and possess detectable levels of HIF1α and ARC expression under normoxia, Caki1 cells can also induce HIF1α and ARC under hypoxia (Fig. 1B). Thus, we tested the colony-forming capacity of Caki1 cells expressing either a shGFP knockdown construct or two shARC knockdown constructs in normoxia (21% O_2) or hypoxia (2% O_2). In response to ARC knockdown, we observed a marked decrease of Caki1 survival under normoxia and hypoxia compared to GFP knockdown (Fig. 5D). In parallel experiments, we compared the growth rate of the same cells under normoxia (21% O_2) and hypoxia (0.5% O_2) for 2 weeks and we found a substantial decrease in the growth of Caki1 cells expressing shARC, particularly under hypoxia (Fig. 5E). Importantly, Caki1 shARC no. 2 cells retained the least amount of ARC compared to Caki1 shARC no. 1, had more cleaved caspase 3 (Fig. 5A), more active caspase (Fig. 5B), more annexin V-positive, PI-negative cells (Fig. 5C), formed the smallest amount of colonies (Fig. 5D), and had the lowest growth rate (Fig. 5E) among the three groups analyzed.

Next, we assessed the role of ARC in RCC chemoresistance. Figure 5F shows that ARC knockdown contributes to chemosensitization of Caki1 cells, and the effect can be rescued by overexpression of shRNA-insensitive ARC cDNA (sh-in-ARC), confirming that the effects are on target (see Materials and Methods for details on construct generation). This result is of particular interest, since RCC-type cancer is notoriously resistant to chemotherapy.

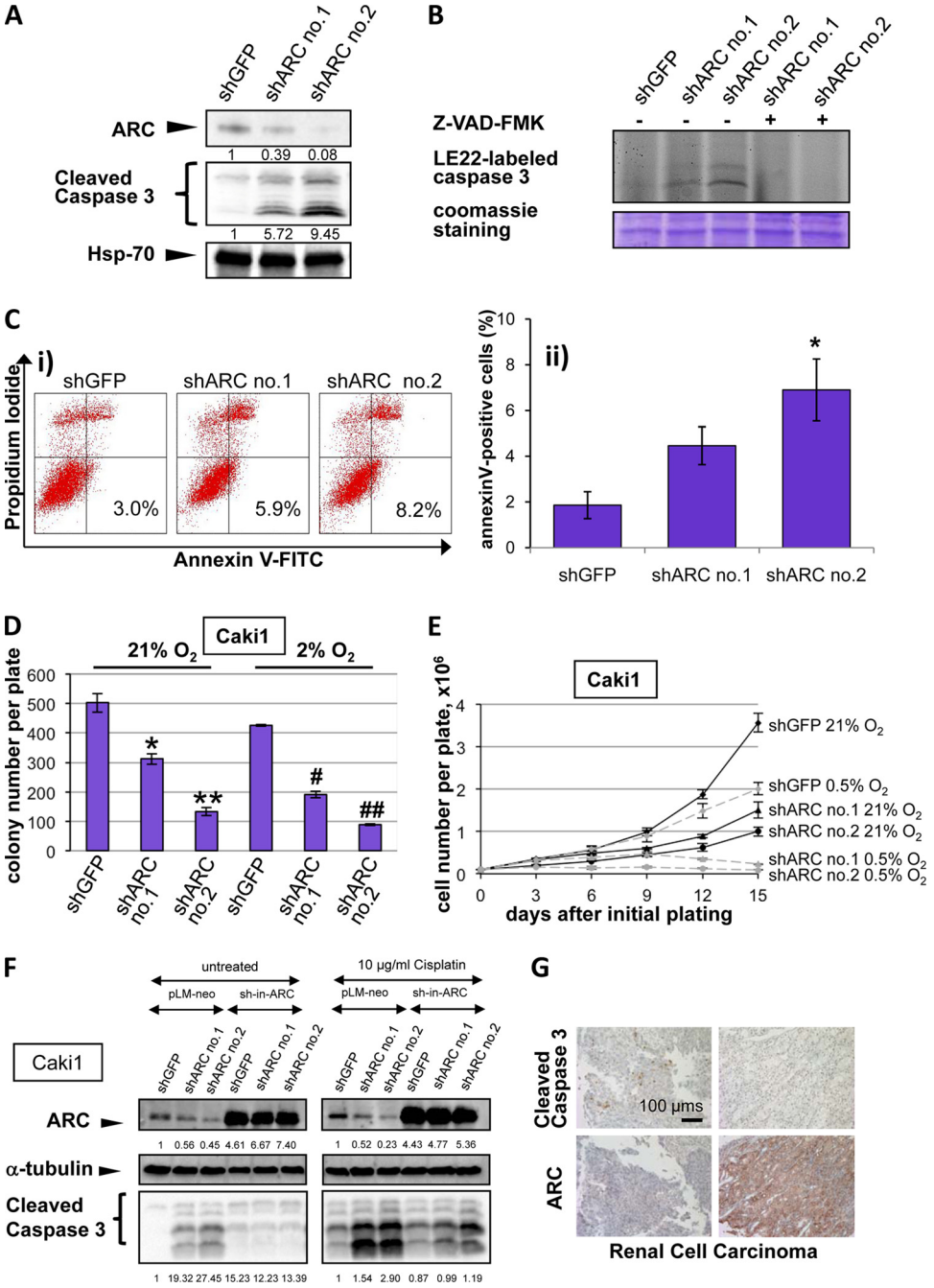

FIG 5 ARC knockdown decreases cell survival and retards cell growth under normoxia and hypoxia. (A) Western blot showing downregulation of ARC expression in Caki1 cells after infection with two shRNA-expressing lentiviral constructs, leading to cleavage of caspase 3. (B) Caspase 3 activity was assessed using the fluorescent probe LE22. We observed binding of the probe to caspase 3 in cells where ARC was knocked down but not in shGFP-infected cells, and binding was abrogated by treatment with caspase inhibitor Z-VAD-FMK. Coomassie-stained gel controls were used for equal protein loading. (C) Caki1 cells stably expressing either shGFP or two different shRNAs targeting ARC were analyzed for apoptosis by flow cytometry. The percentages of annexin V-positive PI-negative cells are indicated. Results of a representative experiment are shown in panel i. Results in panel ii represent the average percent annexin V-positive, PI-negative cells ± SEM from three independent experiments. *, $P = 0.027$. (D) ARC knockdown reduces the colony-forming capacity of Caki1 cells under normoxic and hypoxic conditions. Graphs show the average colony numbers per plate in two independent experiments ± SEM. *, $P < 0.05$; ** and #, $P < 0.01$; ##, $P < 0.001$. * and **, comparison to Caki1 shGFP in normoxia; # and ##, comparison to Caki1 shGFP in hypoxia. (E) ARC knockdown retards cell growth of Caki1 cells under normoxic and especially hypoxic conditions. Cell number per plate (*y* axis) is plotted against days after initial plating at day 0 (*x* axis). Error bars represent standard deviations. (F) ARC knockdown contributes to chemosensitization of Caki1 cells, and the effect can be rescued by overexpression of shRNA insensitive ARC cDNA. Cells were treated with 10 µg/ml cisplatin for 17 h or left untreated, and caspase 3 cleavage was assessed by Western blotting. (G) Examples of ARC-negative and cleaved caspase 3-positive as well as ARC-positive and cleaved caspase 3-negative IHC staining on the RCC TMA. TMA contained just 3 out of 35 spots that were positive for cleaved caspase 3, and all of them were ARC negative. For panels A and F, experiments were performed under normoxia. shRNA targeting green fluorescent protein (shGFP) and the vector pLM-CMV-H4-neo-PL3 were used as controls; Hsp-70 (mitochondrial heat shock protein 70) (A) and α-tubulin (F) are shown as loading controls.

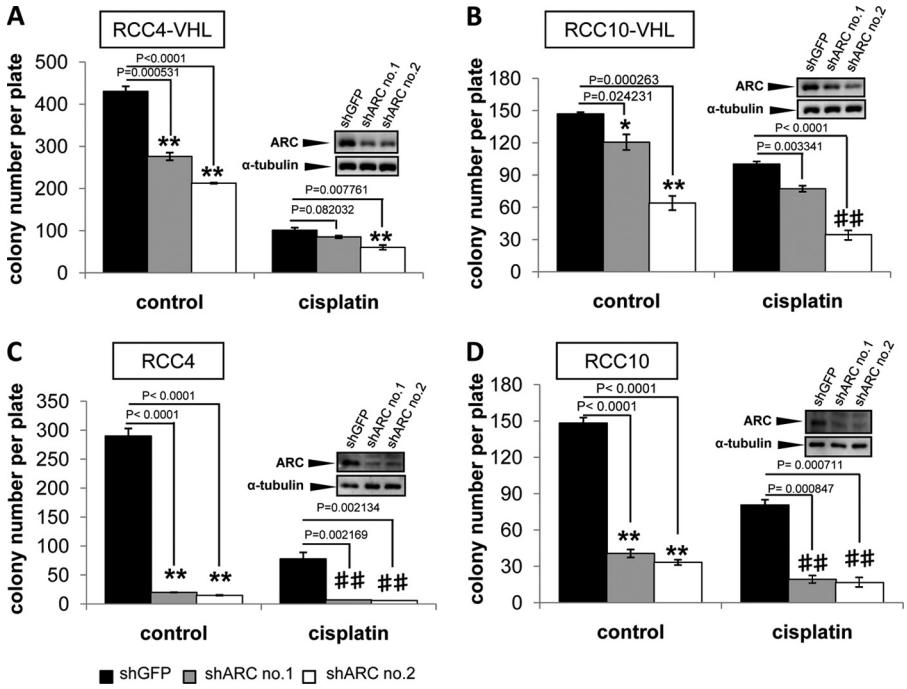

FIG 6 ARC knockdown leads to suppression of colony formation in RCC4 and RCC10 cells with and without VHL, and the effect of knockdown on cell survival is more pronounced in *VHL*-deficient cells. RCC4 and matched RCC4-VHL cells as well as RCC10 and matched RCC10-VHL cells were infected with viruses encoding shRNA targeting GFP (control) and two shRNAs targeting ARC. After selection on puromycin, 12 acquired cell lines were subjected to colony assays. Cells were pretreated with 0.5 μg/ml cisplatin or vehicle treated. This experiment was repeated twice in triplicate.

We also assessed ARC and cleaved caspase 3 staining on the TMA to evaluate if there is a correlation between the two stainings, confirming the role of ARC as an inhibitor of caspase 3 cleavage in human tumors. Although the TMA contained just 3 out of 35 spots positive for cleaved caspase 3, all of them were ARC negative (Fig. 5G). Further studies involving large numbers of tumor samples with different tumor grades and stages are needed to confirm this finding and to draw more definitive conclusions.

Expression of ARC in RCC cell lines confers cell survival and protects them from cisplatin-induced cell death. To evaluate the effect of ARC knockdown on survival of matched RCC cell lines with and without *VHL*, we included four more cell lines in the study. Genetically matched RCC4 and RCC4-VHL cells and RCC10 and RCC10-VHL cells were infected with viruses encoding shRNA targeting GFP (control) and two shRNAs targeting ARC. After selection on puromycin, 12 acquired cell lines were subjected to colony assays. Cells were pretreated with 0.5 μg/ml cisplatin or vehicle treated (control). Figure 6 shows that ARC knockdown leads to suppression of colony formation in RCC4 cells with and without VHL and RCC10 cells with and without VHL, especially when combined with cisplatin treatment, and the effect of knockdown on cell survival is more pronounced in *VHL*-deficient cells.

Caki1 cells with downregulated ARC expression show decreased tumorigenic potential in SCID mice. In light of the effects the downregulation of ARC expression had on survival and growth of renal cancer cell lines *in vitro*, we decided to investigate the effect of ARC inhibition on tumor forming potential in immunodeficient mice. It is important to mention that currently there is no robust mouse model to study RCC primary tumor formation and metastasis. Caki1 cells are a low-*VHL*-expressing cell line and form subcutaneous (s.c.) tumors with long periods of latency and do not metastasize. We used Caki1 cells, which we also used in our *in vitro* work, for *in vivo* studies, since they are low-*VHL*-expressing cells and are frequently used by others for animal studies of RCC (36–38). We injected Caki1 cells stably transduced with shGFP, shARC no. 1, and shARC no. 2 s.c. into the dorsal flanks of SCID mice. After 13 weeks, tumor dimensions were measured with calipers, and tumor volume was calculated. The results clearly showed that ARC expression led to impairment of tumor initiation ability in Caki1 cells (Fig. 7). Nine out of 10 injections of shGFP Caki1 cells grew into tumors. In contrast, only one out of 14 injections of shARC Caki1 cells formed a tumor. These results indicate that elevated levels of ARC in CC-RCC are essential for initiating tumor growth.

DISCUSSION

In this study, we showed that the antiapoptotic protein ARC confers RCC the capacity to maintain their neoplastic phenotype *in vitro* and *in vivo*: ARC downregulation is accompanied by decreased cell survival and impairment of growth *in vitro* and by inhibition of tumor-forming ability *in vivo*. Although ARC regulation at the posttranslational level through ubiquitination and proteasomal degradation was rigorously studied (15, 16), actual factors binding to its promoter and regulating its expression just start to be elucidated. The indirect effects of the Ras/MEK/extracellular signal-regulated kinase pathway on ARC promoter stimulation and of the p53 pathway on ARC promoter repression were previously reported (17, 18), along with a recent report of HIF-dependent ARC regulation (39) (see discussion below). In the present study, we have shown that increased ARC expression is stimulated by direct HIF1 binding to ARC promoter under hyp-

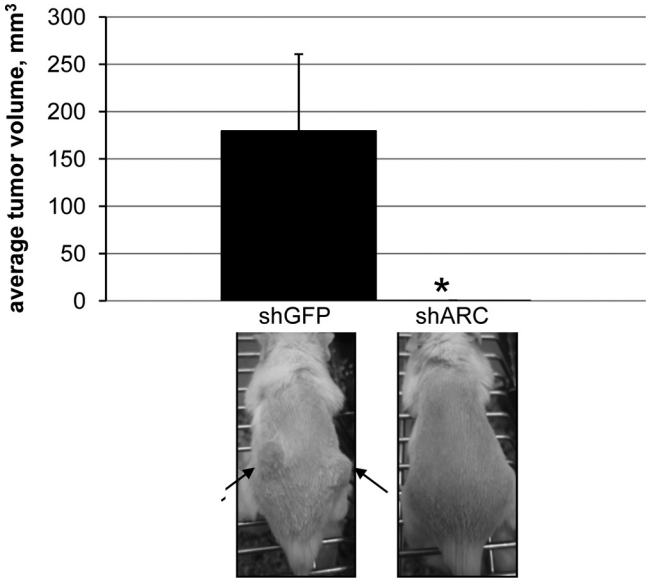

FIG 7 ARC knockdown decreases the tumor-forming ability of Caki1 cells. Caki1 cells stably expressing shGFP, shARC no. 1, or shARC no. 2 shRNA lentiviral constructs were injected s.c. into the right and left flanks of SCID mice. In this analysis, mice in the shARC no. 1 and shARC no. 2 groups were pooled and designated a shARC group. Representative pictures of mice are shown for each group. Average tumor volumes were calculated at the end of the study. *, $P = 0.0153$.

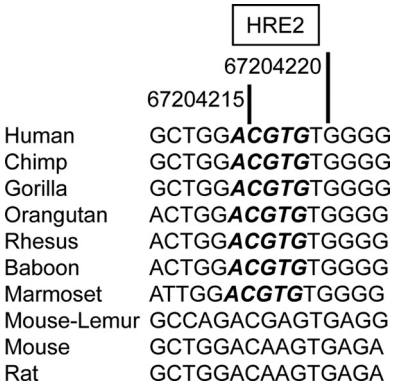

FIG 8 Genomic DNA alignment of regions containing HRE2 HIF binding site in *ARC* promoter among different species, as indicated. The numbers above the sequences correspond to coordinates in the UCSC Genome Browser, human, February 2009 (GRCh37/hg19 assembly).

oxia in cells with WT *VHL* or under normoxia in cells with mutated/lost *VHL*. Solid tumors are known to be invariably less well oxygenated in comparison to their normal tissue of origin, making low oxygen tension, or hypoxia, a critical hallmark of cancer development (40). Our findings of ARC regulation by hypoxia and HIF1 in CC-RCC deserve further investigation in solid tumors of other tissue origin, aiming at better defining the contribution of ARC to tumor cell survival and possibly therapeutic resistance.

The antiapoptotic function of ARC appears to be well conserved in different cell types, including cancer cells as well as cells in normal tissues (14, 41–43). In agreement with our data, ARC was shown to inhibit cell death potently in cancer cells (HeLa, MCF7, and HCT116) (43) and in cardiomyocytes (14, 41, 42). However, the regulation of ARC expression by hypoxia or other injuries (ischemia/reperfusion) shows cell type and/or species specificity. Unlike our observations in a variety of human cancer cell types, hypoxia treatment of rat H9C2 cardiomyocytes and ventricular myocytes led to decreased ARC levels in a manner that correlated with the induction of apoptosis and/or necrosis (41). On the other hand, in the recent report by Zaiman et al., ARC was shown to be induced by hypoxia in isolated rat pulmonary arterial smooth muscle cells (44). Interestingly, the putative HIF1α binding site identified in our study appears to be conserved in primates but is not present in the mouse or rat ARC promoter (Fig. 8). Importantly, we could not detect ARC expression in mouse embryonic fibroblasts (MEFs) under normoxia and hypoxia by Western blotting, which is in line with the fact that MEFs are highly susceptible to apoptotic death under hypoxia (45). Thus, the mechanism of ARC regulation by hypoxia might be complex, and tissue specificity and/or species-specific regulation should be taken into consideration. Studies by Nam et al. (15) and Foo et al. (16) have shown the role of ARC ubiquitination and proteasomal degradation in regulation of its expression at the protein level in cells of rat and mouse origin. Further studies are needed to clarify the contribution of proteasomal degradation and transcriptional upregulation by hypoxia in ARC expression and its subsequent impact on cell survival/proliferation in human cancer.

A recent paper by Ao et al. identified *ARC* as a hypoxia-inducible and HIF1-regulated gene (39), although the study did not investigate if *ARC* is a target gene of HIF1, HIF2, or both. These authors identified the GCGTG motif as a HIF1 binding site, which is different from the ACGTG site identified in our study. The GCGTG site might represent an alternative HIF binding site, and it would be important to assess its conservation in different species.

Our ChIP data clearly showed that HIF1α and HIF2α are capable of binding to HRE2 in the ARC promoter. At the same time, just endogenous HIF1 regulates ARC transcription (Fig. 2), although HIF2 can regulate ARC transcription when exogenously overexpressed (Fig. 3C). This finding once more strengthens the notion that binding to the promoter does not equal activation.

The HIF1 dependence of ARC raises the question as to how a HIF1-regulated gene can have such an essential role in CC-RCC, considering the largely accepted view that it is rather the silencing of HIF2α that is sufficient to impair growth of *VHL*-deficient tumors *in vivo* (46). There is a current debate in the field as to what the roles of the family members HIF1α and HIF2α are in initiation and/or progression of RCC, with an extreme view of the HIF1α gene being a tumor suppressor gene and the HIF2α gene being an oncogene. Indeed, several lines of evidence support this hypothesis, including loss of the HIF1α locus in a number of RCCs, supported by functional studies suggesting that overexpression of HIF1α in *VHL* WT cells restrains tumor growth, whereas suppression of HIF1α in *VHL*-deficient cells enhances tumor growth (reviewed in reference 47). It is important to note that HIFs are transcription factors regulating a large list of target genes, including genes with opposite functions. Thus, tumor-suppressive and oncogenic functions are intrinsic to HIFs, and the shift in their balance will depend on the stage of tumor evolution, as well as the genetic context of a given tumor. We predict that HIF1-mediated antiapoptotic function will be found to be important at early stages of tumor development, when just a few antiapoptotic mechanisms are in play. Later during tumor evolution, more ge-

netic mutations accumulate and more signaling pathways get reprogrammed, allowing multiple mechanisms of apoptosis evasion. At these later stages, the HIF1 antiapoptotic function becomes dispensable, and the balance shifts to more tumor-suppressive functions, leading to selective pressure for HIF1 elimination. A recent and exhaustive study analyzing *VHL* genotype and HIF1α and HIF2α expression in 160 primary renal tumors identified three distinct molecular patterns for human CC-RCCs: those characterized by WT *VHL* and two subtypes with *VHL* deficiencies. Among the latter were tumors typified by both HIF1α and HIF2α induction (H1H2 tumors) and those with exclusive overproduction of HIF2α (H2 tumors) (48). In our study, we found that the ARC gene is a HIF1α-regulated gene which promotes CC-RCC cell survival. Thus, we suggest that ARC might play an essential role in survival of renal cancer cells in some tumors from the first two groups: tumors with *VHL* WT and *VHL*-deficient tumors (H1H2).

Since CC-RCC is highly aggressive and unresponsive to radiation and chemotherapy, there is a large interest in the field concerning the mechanism of this resistance, especially because *p53* mutations are rarely detected in this type of cancer (49) (IARC p53 database [http://www-p53.iarc.fr/]). Several mechanisms of resistance to therapy in relation to p53 have been proposed in the literature: disrupted USP10-mediated deubiquitination of p53 (50), NF-κB-dependent suppression of p53 (51, 52), and HDM2-mediated suppression of p53 (53, 54). Our results suggest an additional mechanism of cell survival in CC-RCC through increased ARC expression. Importantly, ARC was shown to be a negative regulator of p53 function which interferes with p53 tetramerization and stimulates p53 nuclear export (13). Additional research is needed to directly test the role of ARC in the blockade of p53-dependent apoptosis and cell cycle arrest in CC-RCC.

In conclusion, our data suggest that ARC is a promising therapeutic target for *VHL* WT and *VHL*-deficient (H1H2) renal cancers and possibly other types of cancer associated with increased HIF1α activity.

ACKNOWLEDGMENTS

This work was supported by a gift from the Silicon Valley Community Foundation (A.J.G.) and NCI/NIH grants CA-67166 (A.J.G.), CA-088480 (A.J.G.), and T32 CA121940 (O.V.R.).

We thank Giovambattista Pani (Universitá Cattolica del Sacro Cuore, Rome, Italy) for critical reading of the manuscript, Quynh-Thu Le (Stanford) for anti-CAIX antibodies, Alejandro Sweet-Cordero (Stanford) for A549 cells, Marianne Broome-Powell (Stanford) for A375 cells, Silvestre Vicent (Stanford) for pLKO.1shGFP, Peter Chumakov (Case Western Reserve University, Cleveland, OH) for pLM-CMV-H4-puro-PL3 vector, and Aaron Puri (Stanford) for Z-VAD-FMK caspase inhibitor.

REFERENCES

1. **Razorenova OV, Giaccia AJ.** 2010. Hypoxia, gene expression, and metastasis, p 43–58. *In* Bagley RG (ed), The tumor microenvironment. Springer Science+Business Media, LLC, New York, NY.
2. **Semenza GL.** 2009. Regulation of oxygen homeostasis by hypoxia-inducible factor 1. Physiology (Bethesda) **24:**97–106. http://dx.doi.org/10.1152/physiol.00045.2008.
3. **Clark PE.** 2009. The role of VHL in clear-cell renal cell carcinoma and its relation to targeted therapy. Kidney Int. **76:**939–945. http://dx.doi.org/10.1038/ki.2009.296.
4. **Koseki T, Inohara N, Chen S, Nunez G.** 1998. ARC, an inhibitor of apoptosis expressed in skeletal muscle and heart that interacts selectively with caspases. Proc. Natl. Acad. Sci. U. S. A. **95:**5156–5160. http://dx.doi.org/10.1073/pnas.95.9.5156.
5. **Nam YJ, Mani K, Ashton AW, Peng CF, Krishnamurthy B, Hayakawa Y, Lee P, Korsmeyer SJ, Kitsis RN.** 2004. Inhibition of both the extrinsic and intrinsic death pathways through nonhomotypic death-fold interactions. Mol. Cell **15:**901–912. http://dx.doi.org/10.1016/j.molcel.2004.08.020.
6. **Gustafsson AB, Tsai JG, Logue SE, Crow MT, Gottlieb RA.** 2004. Apoptosis repressor with caspase recruitment domain protects against cell death by interfering with Bax activation. J. Biol. Chem. **279:**21233–21238. http://dx.doi.org/10.1074/jbc.M400695200.
7. **Mercier I, Vuolo M, Madan R, Xue X, Levalley AJ, Ashton AW, Jasmin JF, Czaja MT, Lin EY, Armstrong RC, Pollard JW, Kitsis RN.** 2005. ARC, an apoptosis suppressor limited to terminally differentiated cells, is induced in human breast cancer and confers chemo- and radiation-resistance. Cell Death Differ. **12:**682–686. http://dx.doi.org/10.1038/sj.cdd.4401631.
8. **Wang M, Qanungo S, Crow MT, Watanabe M, Nieminen AL.** 2005. Apoptosis repressor with caspase recruitment domain (ARC) is expressed in cancer cells and localizes to nuclei. FEBS Lett. **579:**2411–2415. http://dx.doi.org/10.1016/j.febslet.2005.03.040.
9. **Chen LH, Jiang CC, Watts R, Thorne RF, Kiejda KA, Zhang XD, Hersey P.** 2008. Inhibition of endoplasmic reticulum stress-induced apoptosis of melanoma cells by the ARC protein. Cancer Res. **68:**834–842. http://dx.doi.org/10.1158/0008-5472.CAN-07-5056.
10. **Wang JX, Li Q, Li PF.** 2009. Apoptosis repressor with caspase recruitment domain contributes to chemotherapy resistance by abolishing mitochondrial fission mediated by dynamin-related protein-1. Cancer Res. **69:**492–500. http://dx.doi.org/10.1158/0008-5472.CAN-08-2962.
11. **Medina-Ramirez CM, Goswami S, Smirnova T, Bamira D, Benson B, Ferrick N, Segall J, Pollard JW, Kitsis RN.** 2011. Apoptosis inhibitor ARC promotes breast tumorigenesis, metastasis, and chemoresistance. Cancer Res. **71:**7705–7715. http://dx.doi.org/10.1158/0008-5472.CAN-11-2192.
12. **Carter BZ, Qiu YH, Zhang N, Coombes KR, Mak DH, Thomas DA, Ravandi F, Kantarjian HM, Koller E, Andreeff M, Kornblau SM.** 2011. Expression of ARC (apoptosis repressor with caspase recruitment domain), an antiapoptotic protein, is strongly prognostic in AML. Blood **117:**780–787. http://dx.doi.org/10.1182/blood-2010-04-280503.
13. **Foo RS, Nam YJ, Ostreicher MJ, Metzl MD, Whelan RS, Peng CF, Ashton AW, Fu W, Mani K, Chin SF, Provenzano E, Ellis I, Figg N, Pinder S, Bennett MR, Caldas C, Kitsis RN.** 2007. Regulation of p53 tetramerization and nuclear export by ARC. Proc. Natl. Acad. Sci. U. S. A. **104:**20826–20831. http://dx.doi.org/10.1073/pnas.0710017104.
14. **Neuss M, Monticone R, Lundberg MS, Chesley AT, Fleck E, Crow MT.** 2001. The apoptotic regulatory protein ARC (apoptosis repressor with caspase recruitment domain) prevents oxidant stress-mediated cell death by preserving mitochondrial function. J. Biol. Chem. **276:**33915–33922. http://dx.doi.org/10.1074/jbc.M104080200.
15. **Nam YJ, Mani K, Wu L, Peng CF, Calvert JW, Foo RS, Krishnamurthy B, Miao W, Ashton AW, Lefer DJ, Kitsis RN.** 2007. The apoptosis inhibitor ARC undergoes ubiquitin-proteasomal-mediated degradation in response to death stimuli: identification of a degradation-resistant mutant. J. Biol. Chem. **282:**5522–5528. http://dx.doi.org/10.1074/jbc.M609186200.
16. **Foo RS, Chan LK, Kitsis RN, Bennett MR.** 2007. Ubiquitination and degradation of the anti-apoptotic protein ARC by MDM2. J. Biol. Chem. **282:**5529–5535. http://dx.doi.org/10.1074/jbc.M609046200.
17. **Li YZ, Lu DY, Tan WQ, Wang JX, Li PF.** 2008. p53 initiates apoptosis by transcriptionally targeting the antiapoptotic protein ARC. Mol. Cell. Biol. **28:**564–574. http://dx.doi.org/10.1128/MCB.00738-07.
18. **Wu L, Nam YJ, Kung G, Crow MT, Kitsis RN.** 2010. Induction of the apoptosis inhibitor ARC by Ras in human cancers. J. Biol. Chem. **285:**19235–19245. http://dx.doi.org/10.1074/jbc.M110.114892.
19. **Kondo K, Klco J, Nakamura E, Lechpammer M, Kaelin WG, Jr.** 2002. Inhibition of HIF is necessary for tumor suppression by the von Hippel-Lindau protein. Cancer Cell **1:**237–246. http://dx.doi.org/10.1016/S1535-6108(02)00043-0.
20. **Yan Q, Bartz S, Mao M, Li L, Kaelin WG, Jr.** 2007. The hypoxia-inducible factor 2alpha N-terminal and C-terminal transactivation domains cooperate to promote renal tumorigenesis in vivo. Mol. Cell Biol. **27:**2092–2102. http://dx.doi.org/10.1128/MCB.01514-06.
21. **Razorenova OV, Finger EC, Colavitti R, Chernikova SB, Boiko AD, Chan CK, Krieg A, Bedogni B, LaGory E, Weissman IL, Broome-Powell M, Giaccia AJ.** 2011. VHL loss in renal cell carcinoma leads to up-

regulation of CUB domain-containing protein 1 to stimulate PKC{delta}-driven migration. Proc. Natl. Acad. Sci. U. S. A. **108:**1931–1936. http://dx.doi.org/10.1073/pnas.1011777108.
22. **Krieg AJ, Rankin EB, Chan D, Razorenova O, Fernandez S, Giaccia AJ.** 2010. Regulation of the histone demethylase JMJD1A by hypoxia-inducible factor 1 alpha enhances hypoxic gene expression and tumor growth. Mol. Cell. Biol. **30:**344–353. http://dx.doi.org/10.1128/MCB.00444-09.
23. **Schodel J, Oikonomopoulos S, Ragoussis J, Pugh CW, Ratcliffe PJ, Mole DR.** 2011. High-resolution genome-wide mapping of HIF-binding sites by ChIP-seq. Blood **117:**e207–e217. http://dx.doi.org/10.1182/blood-2010-10-314427.
24. **Razorenova OV, Ivanov AV, Budanov AV, Chumakov PM.** 2005. Virus-based reporter systems for monitoring transcriptional activity of hypoxia-inducible factor 1. Gene **350:**89–98. http://dx.doi.org/10.1016/j.gene.2005.02.006.
25. **Higgins JP, Wang L, Kambham N, Montgomery K, Mason V, Vogelmann SU, Lemley KV, Brown PO, Brooks JD, van de Rijn M.** 2004. Gene expression in the normal adult human kidney assessed by complementary DNA microarray. Mol. Biol. Cell **15:**649–656. http://dx.doi.org/10.1091/mbc.E03-06-0432.
26. **Zhao H, Ljungberg B, Grankvist K, Rasmuson T, Tibshirani R, Brooks JD.** 2006. Gene expression profiling predicts survival in conventional renal cell carcinoma. PLoS Med. **3:**e13. http://dx.doi.org/10.1371/journal.pmed.0030013.
27. **Nicolau M, Tibshirani R, Borresen-Dale AL, Jeffrey SS.** 2007. Disease-specific genomic analysis: identifying the signature of pathologic biology. Bioinformatics **23:**957–965. http://dx.doi.org/10.1093/bioinformatics/btm033.
28. **Edgington LE, van Raam BJ, Verdoes M, Wierschem C, Salvesen GS, Bogyo M.** 2012. An optimized activity-based probe for the study of caspase-6 activation. Chem. Biol. **19:**340–352. http://dx.doi.org/10.1016/j.chembiol.2011.12.021.
29. **An J, Fisher M, Rettig MB.** 2005. VHL expression in renal cell carcinoma sensitizes to bortezomib (PS-341) through an NF-kappaB-dependent mechanism. Oncogene **24:**1563–1570. http://dx.doi.org/10.1038/sj.onc.1208348.
30. **Haase VH.** 2006. Hypoxia-inducible factors in the kidney. Am. J. Physiol. Renal Physiol. **291:**F271–281. http://dx.doi.org/10.1152/ajprenal.00071.2006.
31. **Beroukhim R, Brunet JP, Di Napoli A, Mertz KD, Seeley A, Pires MM, Linhart D, Worrell RA, Moch H, Rubin MA, Sellers WR, Meyerson M, Linehan WM, Kaelin WG, Jr, Signoretti S.** 2009. Patterns of gene expression and copy-number alterations in von-Hippel Lindau disease-associated and sporadic clear cell carcinoma of the kidney. Cancer Res. **69:**4674–4681. http://dx.doi.org/10.1158/0008-5472.CAN-09-0146.
32. **Gumz ML, Zou H, Kreinest PA, Childs AC, Belmonte LS, LeGrand SN, Wu KJ, Luxon BA, Sinha M, Parker AS, Sun LZ, Ahlquist DA, Wood CG, Copland JA.** 2007. Secreted frizzled-related protein 1 loss contributes to tumor phenotype of clear cell renal cell carcinoma. Clin. Cancer Res. **13:**4740–4749. http://dx.doi.org/10.1158/1078-0432.CCR-07-0143.
33. **Lenburg ME, Liou LS, Gerry NP, Frampton GM, Cohen HT, Christman MF.** 2003. Previously unidentified changes in renal cell carcinoma gene expression identified by parametric analysis of microarray data. BMC Cancer **3:**31. http://dx.doi.org/10.1186/1471-2407-3-31.
34. **Potter C, Harris AL.** 2004. Hypoxia inducible carbonic anhydrase IX, marker of tumour hypoxia, survival pathway and therapy target. Cell Cycle **3:**164–167. http://dx.doi.org/10.4161/cc.3.2.618.
35. **Ludwig-Galezowska AH, Flanagan L, Rehm M.** 2011. Apoptosis repressor with caspase recruitment domain, a multifunctional modulator of cell death. J. Cell. Mol. Med. **15:**1044–1053. http://dx.doi.org/10.1111/j.1582-4934.2010.01221.x.
36. **Tsimafeyeu I, Zaveleva E, Stepanova E, Low W.** 2013. OM-RCA-01, a novel humanized monoclonal antibody targeting fibroblast growth factor receptor 1, in renal cell carcinoma model. Invest. New Drugs **31:**1436–1443. http://dx.doi.org/10.1007/s10637-013-0017-x.
37. **Olwill SA, Joffroy C, Gille H, Vigna E, Matschiner G, Allersdorfer A, Lunde BM, Jaworski J, Burrows JF, Chiriaco C, Christian HJ, Hulsmeyer M, Trentmann S, Jensen K, Hohlbaum AM, Audoly L.** 2013. A highly potent and specific MET therapeutic protein antagonist with both ligand-dependent and ligand-independent activity. Mol. Cancer Ther. **12:**2459–2471. http://dx.doi.org/10.1158/1535-7163.MCT-13-0318.
38. **Juengel E, Makarevic J, Tsaur I, Bartsch G, Nelson K, Haferkamp A, Blaheta RA.** 2013. Resistance after chronic application of the HDAC-inhibitor valproic acid is associated with elevated Akt activation in renal cell carcinoma in vivo. PLoS One **8:**e53100. http://dx.doi.org/10.1371/journal.pone.0053100.
39. **Ao JE, Kuang LH, Zhou Y, Zhao R, Yang CM.** 2012. Hypoxia-inducible Factor 1 regulated ARC expression mediated hypoxia induced inactivation of the intrinsic death pathway in p53 deficient human colon cancer cells. Biochem. Biophys. Res. Commun. **420:**913–917. http://dx.doi.org/10.1016/j.bbrc.2012.03.101.
40. **Hockel M, Schlenger K, Knoop C, Vaupel P.** 1991. Oxygenation of carcinomas of the uterine cervix: evaluation by computerized O2 tension measurements. Cancer Res. **51:**6098–6102.
41. **Ekhterae D, Lin Z, Lundberg MS, Crow MT, Brosius FC, III, Nunez G.** 1999. ARC inhibits cytochrome c release from mitochondria and protects against hypoxia-induced apoptosis in heart-derived H9c2 cells. Circ. Res. **85:**e70–e77. http://dx.doi.org/10.1161/01.RES.85.12.e70.
42. **Gustafsson AB, Sayen MR, Williams SD, Crow MT, Gottlieb RA.** 2002. TAT protein transduction into isolated perfused hearts: TAT-apoptosis repressor with caspase recruitment domain is cardioprotective. Circulation **106:**735–739. http://dx.doi.org/10.1161/01.CIR.0000023943.50821.F7.
43. **Zhang YQ, Herman B.** 2008. Expression and modification of ARC (apoptosis repressor with a CARD domain) is distinctly regulated by oxidative stress in cancer cells. J. Cell Biochem. **104:**818–825. http://dx.doi.org/10.1002/jcb.21666.
44. **Zaiman AL, Damico R, Thoms-Chesley A, Files DC, Kesari P, Johnston L, Swaim M, Mozammel S, Myers AC, Halushka M, El-Haddad H, Shimoda LA, Peng CF, Hassoun PM, Champion HC, Kitsis RN, Crow MT.** 2011. A critical role for the protein apoptosis repressor with caspase recruitment domain in hypoxia-induced pulmonary hypertension. Circulation **124:**2533–2542. http://dx.doi.org/10.1161/CIRCULATIONAHA.111.034512.
45. **Graeber TG, Osmanian C, Jacks T, Housman DE, Koch CJ, Lowe SW, Giaccia AJ.** 1996. Hypoxia-mediated selection of cells with diminished apoptotic potential in solid tumours. Nature **379:**88–91. http://dx.doi.org/10.1038/379088a0.
46. **Kondo K, Kim WY, Lechpammer M, Kaelin WG, Jr.** 2003. Inhibition of HIF2alpha is sufficient to suppress pVHL-defective tumor growth. PLoS Biol. **1:**e83. http://dx.doi.org/10.1371/journal.pbio.0000083.
47. **Jonasch E, Futreal PA, Davis IJ, Bailey ST, Kim WY, Brugarolas J, Giaccia AJ, Kurban G, Pause A, Frydman J, Zurita AJ, Rini BI, Sharma P, Atkins MB, Walker CL, Rathmell WK.** 2012. State of the science: an update on renal cell carcinoma. Mol. Cancer Res. **10:**859–880. http://dx.doi.org/10.1158/1541-7786.MCR-12-0117.
48. **Gordan JD, Lal P, Dondeti VR, Letrero R, Parekh KN, Oquendo CE, Greenberg RA, Flaherty KT, Rathmell WK, Keith B, Simon MC, Nathanson KL.** 2008. HIF-alpha effects on c-Myc distinguish two subtypes of sporadic VHL-deficient clear cell renal carcinoma. Cancer Cell **14:**435–446. http://dx.doi.org/10.1016/j.ccr.2008.10.016.
49. **Petitjean A, Mathe E, Kato S, Ishioka C, Tavtigian SV, Hainaut P, Olivier M.** 2007. Impact of mutant p53 functional properties on TP53 mutation patterns and tumor phenotype: lessons from recent developments in the IARC TP53 database. Hum. Mutat. **28:**622–629. http://dx.doi.org/10.1002/humu.20495.
50. **Yuan J, Luo K, Zhang L, Cheville JC, Lou Z.** 2010. USP10 regulates p53 localization and stability by deubiquitinating p53. Cell **140:**384–396. http://dx.doi.org/10.1016/j.cell.2009.12.032.
51. **Gurova KV, Hill JE, Guo C, Prokvolit A, Burdelya LG, Samoylova E, Khodyakova AV, Ganapathi R, Ganapathi M, Tararova ND, Bosykh D, Lvovskiy D, Webb TR, Stark GR, Gudkov AV.** 2005. Small molecules that reactivate p53 in renal cell carcinoma reveal a NF-kappaB-dependent mechanism of p53 suppression in tumors. Proc. Natl. Acad. Sci. U. S. A. **102:**17448–17453. http://dx.doi.org/10.1073/pnas.0508888102.
52. **Gurova KV, Hill JE, Razorenova OV, Chumakov PM, Gudkov AV.** 2004. p53 pathway in renal cell carcinoma is repressed by a dominant mechanism. Cancer Res. **64:**1951–1958. http://dx.doi.org/10.1158/0008-5472.CAN-03-1541.
53. **Warburton HE, Brady M, Vlatkovic N, Linehan WM, Parsons K, Boyd MT.** 2005. p53 regulation and function in renal cell carcinoma. Cancer Res. **65:**6498–6503. http://dx.doi.org/10.1158/0008-5472.CAN-05-0017.
54. **Roberts AM, Watson IR, Evans AJ, Foster DA, Irwin MS, Ohh M.** 2009. Suppression of hypoxia-inducible factor 2alpha restores p53 activity via Hdm2 and reverses chemoresistance of renal carcinoma cells. Cancer Res. **69:**9056–9064. http://dx.doi.org/10.1158/0008-5472.CAN-09-1770.